Shock Waves
DOI 10.1007/s00193-008-0128-z

ORIGINAL ARTICLE

Numa Manson on velocity deficits and detonation stability

An invited memorial lecture presented at ICDERS 21

S. B. Murray

Received: 30 September 2007 / Accepted: 12 February 2008

Abstract This memorial paper pays tribute to Professor Numa Manson's contributions to the understanding of detonation velocity deficits and wave stability. Manson and his colleague Guénoche postulated that a velocity deficit exists in a tube because the chemical reactions are inhibited in a thin layer adjacent to the tube walls. The hydrodynamic theory of detonation was modified to account for this, and it was shown that the deficit varies inversely with the tube diameter. Manson and his students measured detonation velocities in tubes of various diameter. An estimate of the detonation velocity for an infinite tube diameter was obtained by plotting the velocity against the reciprocal of the tube diameter, ϕ^{-1}, and extrapolating the line through the data to $\phi^{-1} = 0$. The relative contributions of tube geometry and surface roughness to the deficits were systematically studied. Manson was also one of the early investigators to shed light on the cellular structure of detonation by reporting "vibratory phenomena" seen as striations in streak schlieren photographs. An attempt was made to relate this phenomenon to "dispersions" in the propagation velocity and hence the wave stability. The author has extended Manson's work by investigating detonations in tubes with yielding walls. Whereas boundary layers were responsible for the gasdynamic expansion and deficits in Manson's rigid tubes, it was the moving boundaries that caused similar effects in the author's investigations. The author has repeated the "nozzle" analysis of Fay and Dabora using the detonation cell length as the relevant chemical kinetic length scale, and found reasonable agreement between his experimental results and the model. When the Poitiers data are reinterpreted in light of the modified model, the trends are described quite well. More recent studies have shown that the measured deficits for mixtures characterized by irregular cellular structures do not agree with the Fay–Dabora model. Possible reasons for the discrepancy are discussed.

Keywords Gaseous detonation · Velocity deficits · Detonation stability · Cellular structure

PACS 47.40.Rs

Communicated by L. Bauwens.

This paper is based on the invited lecture that was presented at the 21st International Colloquium on the Dynamics of Explosions and Reactive Systems, Poitiers, France, July 23-27, 2007.

S. B. Murray (✉)
DRDC Suffield, P. O. Box 4000,
Station Main, Medicine Hat, AB, Canada T1A 8K6
e-mail: Stephen.Murray@drdc-rddc.gc.ca

1 The Poitiers investigations of velocity deficits

Professor Manson and his students studied velocity deficits and velocity fluctuations in rigid tubes in great detail.

The earliest theoretical prediction for the velocity deficits in tubes was by Zeldovich [41] in 1940. He proposed that the drag exerted on the wall by the fluid between the shock and Chapman–Jouguet (C–J) plane was responsible for the deficits. The model showed that the deficits increased with decreasing tube diameter for a given mixture, but it underpredicted their magnitude considerably. The work on high explosives by Jones [16] and by Eyring et al. [12] arrived at a similar conclusion, but it was the lateral expansion of the gases following the rupture of the charge casing that was proposed to be responsible for energy losses and the associated velocity deficits. Kistiakowsky et al. [17] made precise detonation velocity measurements for a variety of combustible mixtures and showed that the velocity decreases with decreasing tube diameter and varies linearly with the reciprocal of the tube diameter.

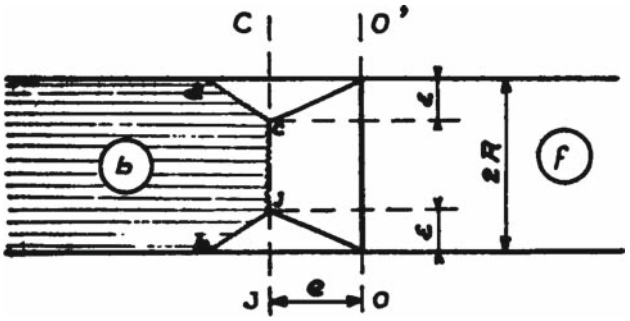

Fig. 1 Model of the detonation wave with wall effects proposed by Manson and Guénoche [25]; reproduced with permission of the Combustion Institute

Professor Manson and his colleague Guénoche [25] proposed yet another hypothesis. They postulated that chemical reactions in the reaction zone of the wave were inhibited or significantly modified in a layer of thickness ϵ adjacent to the tube walls. An attempt was made to modify the hydrodynamic theory of detonation by assuming different heats of reaction in the wall layer and the circular core of radius $R-\epsilon$, where R is the tube radius. The basic wave concept is illustrated in Fig. 1. As ϵ tends to R, the reaction is such that the detonation wave can no longer be maintained and propagation ceases. Thus, the limiting tube diameter $2R_l$ approaches a value of 2ϵ in the limit. In their analysis, an approximate relation between the detonation velocity and heat of reaction was obtained using the Chapman–Jouguet method to yield:

$$D = D_{\text{th}} \cdot \sqrt{\left(1-\frac{\epsilon}{R}\right)^2 + \left[1+\left(1-\frac{\epsilon}{R}\right)^2\right]\left(\frac{D_l}{D_{\text{th}}}\right)^2} \quad (1)$$

where D is the wave velocity in a tube of radius R, D_{th} is the theoretical Chapman–Jouguet velocity, and D_l is the limiting wave velocity when ϵ tends toward R; that is, when the charge diameter becomes equal to the limiting diameter $2R_l$. For $R \gg R_l$ and $\epsilon \cong R_l$, the above expression can be simplified to the following:

$$D \cong D_{\text{th}}\left(1-\frac{R_l}{R}\right) \quad (2)$$

which again shows an increasing velocity deficit with decreasing tube diameter. These investigators tested their hypothesis using the data from experiments in round tubes for C_2H_2–O_2 and C_3H_8–O_2 mixtures at various fuel/oxygen ratios. An important outcome of their work was the conclusion that the detonability limits were not simply a function of the mixture properties alone. The specification of the lower and upper concentration limits must be accompanied by an associated tube diameter. In their own words, "to determine the lower and upper limits of detonation, C_i and C_s, means that we are really determining the limiting diameters for mixtures of concentrations C_i and C_s."

Manson and his students exploited the linear relation between the detonation velocity and the reciprocal of the tube diameter, as first reported by Kistiakowsky et al. [17], in order to estimate the detonation velocity, D_∞, in an infinite diameter tube. Basically, the velocity of detonation, D, for a given mixture at specified initial conditions was measured in several tubes of different diameter, ϕ. D_∞ was then obtained by extrapolating a straight line through the data points to a value of $\phi^{-1} = 0$. The validity of the C–J criterion was then assessed by comparing D_∞ to the theoretical C–J velocity.

The above-described method was employed by a number of Manson's students. Brochet [2], for example, conducted a series of tests using stoichiometric C_3H_8–O_2 and C_2H_4–O_2 mixtures with nitrogen dilution at atmospheric pressure for N_2/O_2 ratios ranging from 0 to 3.76 (corresponding to air). Steel tubes having inside diameters of 6, 12, 21, 36, and 52 mm were employed. The detonation velocities were measured using ionization probes. D_∞ was estimated for a given degree of nitrogen dilution and was found to increase as the dilution decreased. The influence of initial pressure on the detonation velocity was studied in a second set of tests using tubes of 4.6, 28, and 44 mm diameter and initial pressures up to about 300 kPa. When the method was applied to these data, D_∞ was found to increase with increasing initial pressure.

Pujol [33] later extended the D_∞ pressure-dependence work using stainless steel tubes and the same mixtures, but he included C_3H_8–C_2H_4–H_2–O_2 mixtures as well. The dependence of the detonation velocity on initial temperature for temperatures up to 450 K and for various combinations of initial pressure and temperature was also studied. Tubes of 12.5 and 53 mm were used for this purpose. Here, the detonation velocity was observed to decrease with increasing temperature. Pujol also found that the internal surface finish of the tube had a definite influence on the slope of the line in the $D(\phi^{-1})$ plot, but he did not quantify the effect.

Boislève [1] was the first student to apply the method to tubes of rectangular cross section. The tubes in this investigation were brass and they possessed a polished or "mirror" finish. Tubes measuring 10×23, 22×48, and 34×72 mm in cross section were utilized. A "reference diameter" (essentially, the hydraulic diameter) was calculated for each tube. The mixtures employed were stoichiometric C_3H_8–O_2 and C_2H_4–O_2 at initial pressures of 20, 30, 40.5, and 51 kPa. D_∞ was estimated for each initial pressure condition and always found to be somewhat larger than the value for D_∞ obtained for round steel tubes. The values were systematically higher by about 1% for C_3H_8–O_2 and 0.4% for C_2H_4–O_2 mixtures. Boislève also applied the method to estimate the detonation pressure, P_b, for an infinite size tube by plotting P_b as a function of ϕ^{-1} and extrapolating to $\phi^{-1} = 0$. The

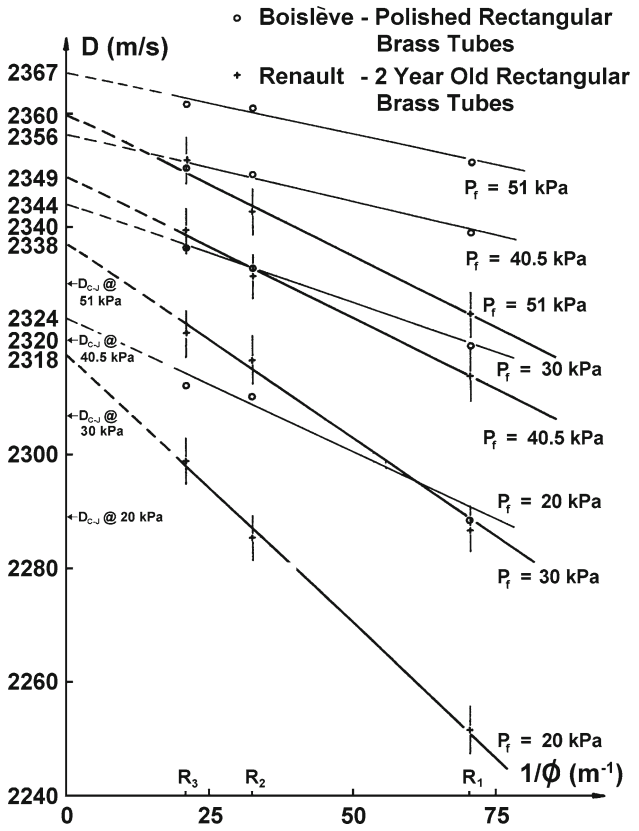

Fig. 2 Detonation velocity versus ϕ^{-1} for polished and rough brass tubes of rectangular cross section for stoichiometric C_3H_8–O_2 mixtures at 292 K [34]. The *arrows* along the *vertical axis* indicate the theoretical detonation velocity for each initial pressure; courtesy of G. Renault

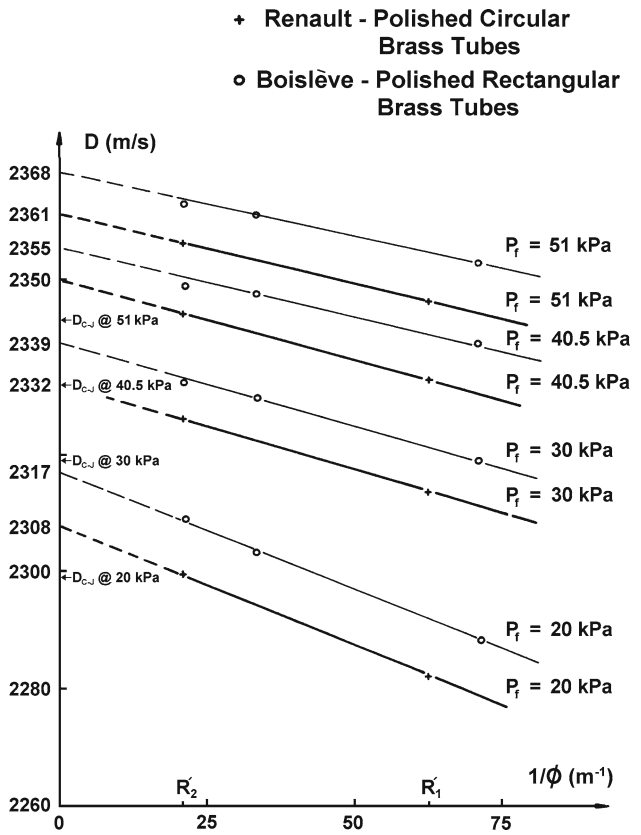

Fig. 3 Detonation velocity versus ϕ^{-1} for polished brass tubes of circular and rectangular cross section for stoichiometric C_2H_4–O_2 mixtures at 292 K [34]. The *arrows* along the *vertical axis* indicate the theoretical detonation velocity for each initial pressure; courtesy of G. Renault

estimated pressures were found to be a few percent higher than P_{C-J}, but they were lower than those estimated for round tubes.

Renault [34] attempted to clarify the respective roles of tube cross section and surface finish on the estimation of D_∞ in two carefully designed sets of experiments building on the earlier work of his colleagues. In the first series of tests, the same three rectangular brass tubes employed by Boislève were used. However, after two years of prior use, the original mirror finish had disappeared and the tubes were noticeably rough. When the tests were repeated for stoichiometric C_3H_8–O_2 at the same initial pressures, the measured propagation velocities for all initial pressures were notably lower than those reported earlier by Boislève. The slopes of the lines in the $D(\phi^{-1})$ plots were also considerably steeper and the resulting D_∞ values were lower. These trends are shown for the propane–oxygen system in Fig. 2. The steeper slopes were likely due to the increased tube roughness playing a more significant role in the case of the smaller tubes. The second series of experiments was conducted with brass tubes of circular cross section (16 and 48 mm diameter) having the same mirror finish as Boislève's original rectangular brass tubes. When the $D(\phi^{-1})$ plots were compared to those for the polished rectangular tubes used by Boislève, the slopes were nearly identical for a given initial pressure, but the velocities were ∼5–10 m/s lower for the circular tubes. Figure 3 shows typical results for the ethylene–oxygen system. Given that the surface finishes were identical, the differences in D_∞ for a given initial pressure were clearly due to geometrical effects. For both tube geometries, the slopes of the lines steepen as the wall roughness increases; polished surfaces yield the minimum slope, while rough surfaces give the highest slope. The value of D_∞ therefore depends on both the tube cross-sectional geometry and the surface roughness. A compilation of some key results from Manson's students appears in Fig. 4 for low-pressure propane–oxygen.

Brossard and Charpentier de Coysevox [3] tried later to apply the method to responding PVC tubes, but they obtained results considerably different from those for rigid tubes. An attempt to explain the velocity deficits in terms of the energy transferred to the tubes through elastic deformation met with limited success.

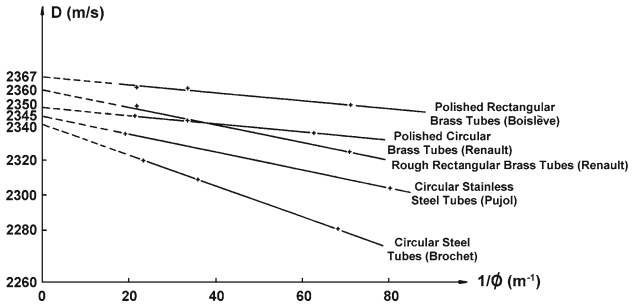

Fig. 4 A compilation of detonation velocity results for tubes of rectangular and circular cross section having various surface finishes. The mixtures were C_3H_8–O_2 at 292 K and 51 kPa [34]; courtesy of G. Renault

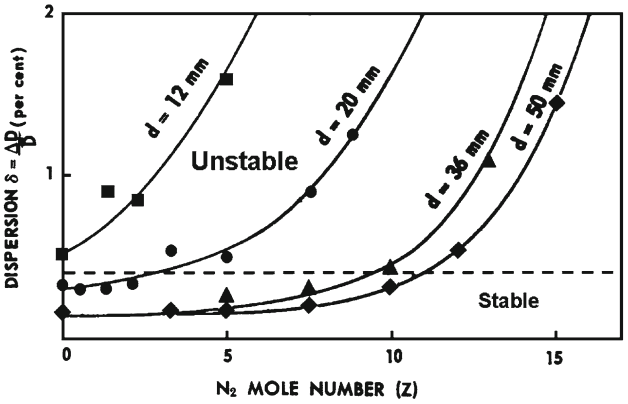

Fig. 5 Relative dispersion, δ, versus nitrogen mole number, Z, for $C_3H_8 + 5O_2 + ZN_2$, $P_o = 101.3$ kPa and $T_o = 298$ K [24]; reproduced with permission of the Combustion Institute

2 The Poitiers investigations of "vibratory phenomena" and wave stability

Manson [23] first reported that gaseous detonations in round tubes exhibit "vibratory phenomena" during the mid 1940s. He proposed that the frequency of these vibrations was equal to the fundamental transverse acoustic frequency of the tube. When experiments were conducted for $CO + 0.5O_2$ mixtures in rigid tubes ranging in diameter from 0.362 to 2.54 cm, the frequency of luminous striations observed in streak photographs was found to be in excellent agreement with the predicted acoustic frequency of the tube. The same conclusion was reached for H_2–O_2, C_2H_2–O_2, and CH_4–O_2 mixtures in tubes up to 4.1 cm in diameter. The experiments also showed that the vibrational frequency was inversely proportional to the tube diameter. In some experiments, higher vibrational frequencies were observed, and these were shown to correspond to the second acoustic frequency of the tube. In a later investigation [24], an attempt was made to relate the local propagation velocity of the wave to the vibratory phenomena. In that study, experiments were carried out in round steel tubes 25–30 m long having diameters of 6, 12, 14.6, 20, 28, 36, 44, and 52 mm. The combustible mixtures were nitrogen-diluted C_3H_8–O_2 and C_2H_4–O_2 for a range of equivalence ratios and degrees of dilution. The propagation velocities were measured using ionization probes, while the vibratory phenomena were recorded using a streak schlieren system. The "local" detonation velocity, D_l, was defined as that measured over a distance of 0.5 m, while the "average" velocity, D_m, was that measured over a distance of at least 5 m. Care was taken to ensure that the measurements were not influenced by the initiator.

The velocity "dispersion," δ, was defined as $\Delta D/\bar{D}$ where ΔD is the maximum deviation between D_l and D_m, and $\bar{D}$ is the average of these velocities, $(D_l + D_m)/2$. The experimental results showed that for any given mixture, δ increases as the tube diameter, d, decreases. Equivalently, for a given tube and stoichiometric ratio, δ increases as the degree of dilution increases. Figure 5 shows the measured velocity dispersions for $C_3H_8 + 5O_2 + ZN_2$ mixtures with $0 \leq Z \leq 14.7$. A value of δ less than 0.4% was deemed to be insignificant and the wave was considered to be "stable". The data indicate that δ becomes larger than 0.4% for $Z = 3.5$ in the 20-mm tube, $Z = 9$ in the 36-mm tube, and $Z = 10.5$ in the 52-mm tube. These tests showed that the detonation reaction zone must be lengthened (through nitrogen dilution) as the tube diameter increases in order for local velocity dispersions and the onset of instability to become apparent.

Figure 6 is a collection of streak schlieren photographs showing vibratory phenomena for $C_3H_8 + 5O_2 + ZN_2$ mixtures with varying degrees of N_2 dilution. For low values of Z, very high frequency vibrations were observed in the burned gases accompanied by low values of velocity dispersion. As the value of Z increased, the velocity dispersions increased and the striations in the photographs eventually appeared at a frequency equal to the fundamental frequency of the transverse vibrations. At some higher value of Z, the detonation was seen to decelerate and the shock and flame separate. This was followed by detonation reformation some time later, a process that repeated every 50–60 mm. Each reformation was accompanied initially by high-frequency striations followed by a step-wise transition to the fundamental frequency that persisted for a short time before the next shock/flame decoupling took place. The authors concluded that the increasing instability of the detonation was related to the increasing velocity dispersions, and that the C–J representation of a detonation was only valid for stable detonations, defined as those for which D_l and D_m agreed to within $\pm 0.2\%$. They also proposed that the mode number of the transverse oscillations might be a suitable scale of intrinsic instability.

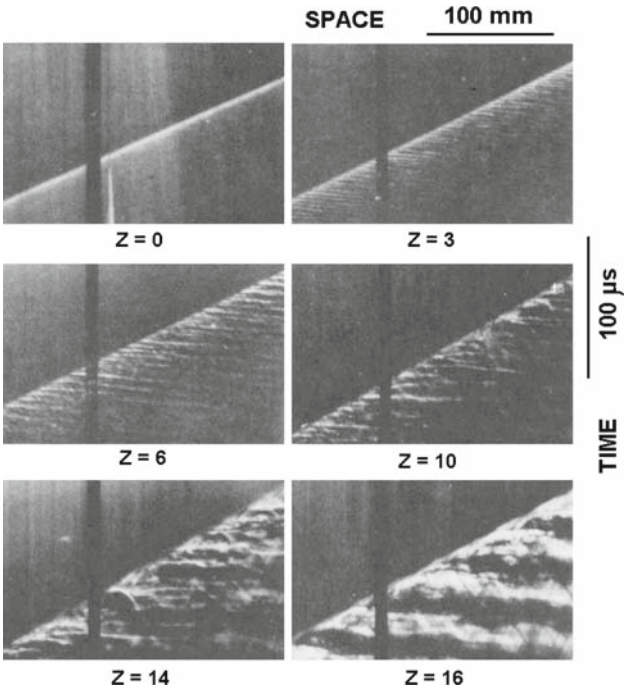

Fig. 6 Streak schlieren photographs of detonations showing instability evolution in $C_3H_8 + 5O_2 + ZN_2$ mixtures as Z increases; $d = 20$ mm, $P_o = 101.3$ kPa, $T_o = 298$ K [24]; reproduced with permission of the Combustion Institute

3 Cellular structure: the true nature of the detonation front revealed

It was once thought that spinning detonations, as first reported by Campbell and Woodhead [4] in the mid 1920s, were an anomaly seen only near the detonability limits. However, during the late 1950s, it became evident that spinning detonation was a limiting case of the universal cellular structure of detonation. Denisov and Troshin [7] used smoke foils to record this structure in the Soviet Union, while White [40] in the United States obtained interferometric photographs showing the non-steady "turbulent" nature of detonation. Although they did not realize it at the time, the vibratory phenomena observed as striations in the streak schlieren photographs by Manson and his coworkers were merely another expression of the cellular character of detonation waves. It took the community some time to inter-relate the various experimental observations and to formulate a coherent picture of the wave front. During the 13th Symposium on Combustion in 1970, Professor Oppenheim chaired a panel discussion in which Professors Manson and Strehlow presented their current views on detonation [26]. Professor Manson emphasized that, "*Above all, the front of the detonation wave is not planar.* In fact, it never appears as a single shock wave, but is made out of a system of oblique shock waves of different intensities, as a consequence of which the combustion front is not planar and the motion of the combustion front is not unidirectional." Professor Strehlow presented smoke foils showing the formation and extinction of transverse waves during the propagation of H_2–O_2–Ar detonations from one mixture to another and stated, "It is hoped that observations of both the appearance and disappearance of transverse waves will allow us to gain more insight into the mechanism which causes their occurrence on propagating detonations."

A plethora of studies during the succeeding decade attempted to understand the intricacies of the cellular structure and to measure the cell sizes for various fuel–oxidizer–diluent systems [22,37].

4 The impact of Manson's work on the author's research

When the author began his fundamental work on gaseous detonation, it was readily appreciated by researchers in the field that the critical conditions for detonation propagation, as well as the velocity deficits during supercritical propagation, were the consequence of an intimate competition between the post-shock rates of gasdynamic expansion and chemical energy release occurring within the detonation front. The rate of expansion depends on the nature of the boundaries defining the physical system (e.g., shape and dimensions of the geometry, compressibility or motion of walls, viscous boundary layer growth, etc.). The rate of energy release depends on the physical and chemical properties of the mixture that are responsible for the complex makeup of the front. In the case of the experiments in rigid tubes conducted in Manson's laboratory, it was the boundary layers that were responsible for the expansion imposed on the wave and the resulting velocity deficits.

Fay [13], and later Dabora et al. [6], had used the elemental induction-zone length as the characteristic wave thickness in their "nozzle" analyses to estimate the velocity deficits. In those analyses, the increase in the area of the post-shock "stream tube," ξ, evaluated over some distance, Δ, deemed to be characteristic of the global rate of chemical reaction, was proposed to be the cause of the observed velocity deficits. However, the deficits predicted by Fay were significantly smaller than those observed, suggesting that the elemental induction-zone length was not an appropriate choice for Δ. In other studies, a calculated "chemical relaxation distance" or the "gross thickness" of the front estimated from schlieren photographs was employed.

Since these early efforts, the universal cellular character of detonation had been revealed and a few correlations suggested that the controlling chemical kinetic length was on the order of the detonation cell size. Mitrofanov and Soloukhin [28] had proposed correlations linking the critical tube diameter, d_c, and the critical channel width, w_c, to the cell width, λ. It had also been shown by Edwards et al. [10] that reinitiation of a diffracting wave commences at a fixed multiple of cell widths from an abrupt area change. Perhaps, now

Fig. 7 Apparatus used for the study of critical conditions, velocity deficits, and detonation stability [31,32]

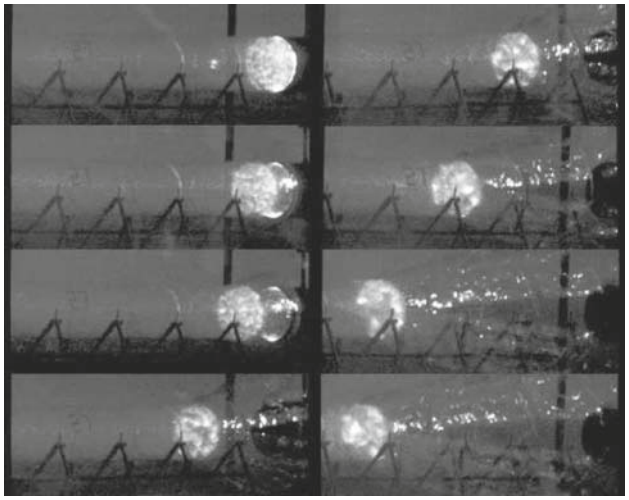

Fig. 8 Cine frames showing propagation of detonation in a 10-mil plastic tube for 3.90% ethylene–air; $D/\lambda \cong 4.1$ [31,32]

that a reasonably well-defined global chemical kinetic length scale had been identified, the stream tube concept warranted renewed consideration. The author's work on critical conditions and velocity deficits is described in Sects. 4.1 and 4.2, respectively. The velocity deficit results of Professor Manson's students are discussed in the context of the author's findings in Sect. 5.

4.1 Critical conditions, stability, and velocity deficits for yielding tubes

4.1.1 Experimental details

In these experiments, the gasdynamic expansion imposed on the wave is due to the wall motion, as opposed to the boundary layers in Manson's work. Ethylene–air detonations were observed propagating in seamless, extruded, polyethylene tubes of 0.89-m diameter. In most tests, an established detonation in a 7.82-m long steel driver of the same diameter was allowed to transmit to the polyethylene tube. The detonation in the driver was initiated using either a high-explosive charge or a 1.5-m long slug of oxyacetylene. In selected tests, the driver was not used and initiation of detonation was brought about instead by a high-explosive charge positioned at one end of the tube, as shown in Fig. 7.

The rate of expansion imposed on the wave was controlled by varying the thickness of the polyethylene wall (1, 5, or 10 mil, where a mil is 0.0254 mm). The wall material surface densities are given in Table 1. The rate of chemical reaction, i.e., the detonation cell size, was controlled by adjusting the mixture composition. Composition and homogeneity of the mixture were monitored by an infrared analyzer to produce a mixture within $\pm 0.05\%$ C_2H_4 of the target concentration. The diagnostic methods included pressure transducers and ionization probes. The pressures and velocities from these sensors confirmed success or failure of propagation and yielded velocity data in cases of successful propagation. The detonation structure was recorded near the driver exit using smoked foils. Cinematographic records were obtained using high-speed cameras. The experimental procedure was to carry out 'Go'–'No-Go' tests for a given polyethylene wall thickness until the critical mixture composition had been identified. The process was then repeated for the other wall thicknesses. Complete details are provided elsewhere [31,32].

4.1.2 Experimental results

Selected frames from a high-speed cine record, showing successful transmission of detonation from the driver and subsequent propagation in the yielding tube, are presented in Fig. 8. The luminous front has a "texture" attributable to the

Table 1 Summary of critical conditions for propagation of C_2H_4–air detonations in circular tubes with yielding walls

Nominal wall thickness t (mil)	Critical C_2H_4 concentration (%)	Theoretical detonation velocity V_{C-J} (m/s)	Mass of yielding wall m/A (kg/m^2)	Critical cell length Lc (mm)	Critical stream tube area increase ξ(%)
1	4.70	1,696	0.0242	129	17.6
5	4.15	1,637	0.124	236	22.3
10	3.90	1,606	0.220	313	23.2

cellular structure of the wave. It can be seen that the scale of this texture increases as the wave enters the yielding confinement as a result of the increased reaction-zone length brought about by the lateral expansion. Conditions in this test were marginal, as evidenced by the spinning behaviour of the wave toward the end of the tube. These observations are reminiscent of the striations observed in Manson's streak schlieren photographs. The detonation becomes noticeably unstable as critical conditions are approached. In the case of the smallest wall thickness, each time the wave propagated over one of the support hoops, the perturbation was sufficient to cause local failure and subsequent re-establishment of detonation in a manner similar to the decoupling and explosive recoupling phenomena reported by Manson in rigid tubes. In one test for which a driver was not used, the initiated wave was seen to propagate steadily for 15 tube diameters, and then fail abruptly upon encountering the first support hoop.

According to Fay [13], the subsonic flow in the globally steady (in shock-fixed coordinates) reaction zone adjusts so that each stream tube experiences the same fractional increase in area between the frontal shock and any location behind the shock before the sonic plane. For the present yielding wall configuration, this means that the relative stream tube area increase for each annular stream tube is equal to that for the yielding tube itself. The latter can be calculated knowing the wall trajectory. For this purpose, a cylindrical piston analogy was adopted in which the piston is the yielding wall material and the driving force is the pressurized gas in the post-shock region of the detonation wave. Complete details are available in Ref. [31,32]. The cell length, L_c, is calculated using the correlation, $d_c = 13\lambda$, linking the cell width to the critical tube diameter, d_c, and a cell aspect ratio, $\lambda/L_c = 0.7$. The correlation for d_c proposed by Moen et al. [30] for C_2H_4-air mixtures is then used: $d_c = ku_s[O_2]^a[C_2H_4]^b \exp(E/RT)$ where u_s, $[O_2]$, $[C_2H_4]$, and T are the post-shock relative particle velocity (m/s), the oxygen and ethylene concentrations (moles/l) and the temperature (K) behind a shock of C–J strength. The exponents a and b are taken from the proposed induction-time formula of Hidaka et al. [15]. A two-parameter fit to the experimental data is then used to yield the kinetic rate factor, $k = 5.65 \times 10^{-7}$s $\cdot$ mole/m^3, and the effective activation energy, $E = 155.7$ kJ/mole, respectively. The results of this exercise, summarized in Table 1, show that the critical conditions for propagation are characterized by a value for ξ near 20% for all three wall thicknesses employed, suggesting that the nature of the critical chemical-gasdynamic balance is identical for the various degrees of confinement.

Under supercritical conditions, the wave propagates with a velocity deficit that is a function of the gasdynamic expansion imposed on the wave. The deficit can be predicted using Dabora et al's [6] version of Fay's "nozzle" analysis [13] and using the detonation cell length once again as the characteristic reaction-zone length. The resulting expression for the deficit is:

$$\frac{\Delta V}{V_{C-J}} = 1 - \left[\frac{(1-\nu)^2}{(1-\nu)^2 + \gamma_2^2(2\nu - \nu^2)} \right]^{1/2}, \tag{3}$$

where $\nu = \xi/(1+\gamma_2)/(1+\xi)$. Here, γ_2 is the ratio of specific heats (or calorific capacities) of the detonation products.

In the case of the 10 mil wall thickness, the support hoops for the tube did not perturb the wave noticeably as critical conditions were approached. The measured velocity deficit under marginal conditions was approximately $10 \pm 2\%$, in good agreement with the value of 9.5% given by Eq. (3) using the critical value for ξ in Table 1. The measurement of velocity deficits near critical conditions for the 1 and 5 mil wall thicknesses was not possible because of the undulating motion of the wave induced by the support hoops.

4.2 Critical conditions and velocity deficits for rigid/yielding channels

4.2.1 Experimental details

A second series of experiments was carried out in the laboratory to investigate the universality of the 20% critical area increase criterion, and to measure velocity deficits under supercritical conditions for a different range of chemical-kinetic and gasdynamic-expansion time scales [31,32]. The apparatus (Fig. 9) was designed to avoid disturbances of the type caused by the support hoops in the large-scale experiments. It consisted of an initiator section, a linear detonation tube, and a test section. The initiator section was filled with equimolar oxyacetylene. The detonation tube and test section were of square cross section (62×62 mm) and contained a nitrogen-diluted C_2H_2–O_2 mixture. All tests were conducted at atmospheric pressure. A ball valve separated the mixtures until moments before ignition. Following spark ignition, the resulting detonation in the initiator section transmitted through the open ball valve to the test mixture in the linear tube. After equilibrating over a 1.64-m length, the wave emerged into one of three interchangeable test sections. In one test section, a single steel wall had been milled from the tube leaving a three-sided channel. A pair of parallel walls had been removed in the second test section. Three walls had been machined away in the third test section, leaving rigid confinement on only one side.

Each rigid boundary that had been removed was replaced by one of five thin yielding materials (see Table 2) including: a paraffin coated paper (Paper A), a common variety of stationery paper (Paper B), a polyethylene plastic, and two types of high-strength acetate plastic (Acetates A and B). Most experiments employed Paper A or Acetate A. Using this apparatus, the rate of gasdynamic expansion imposed

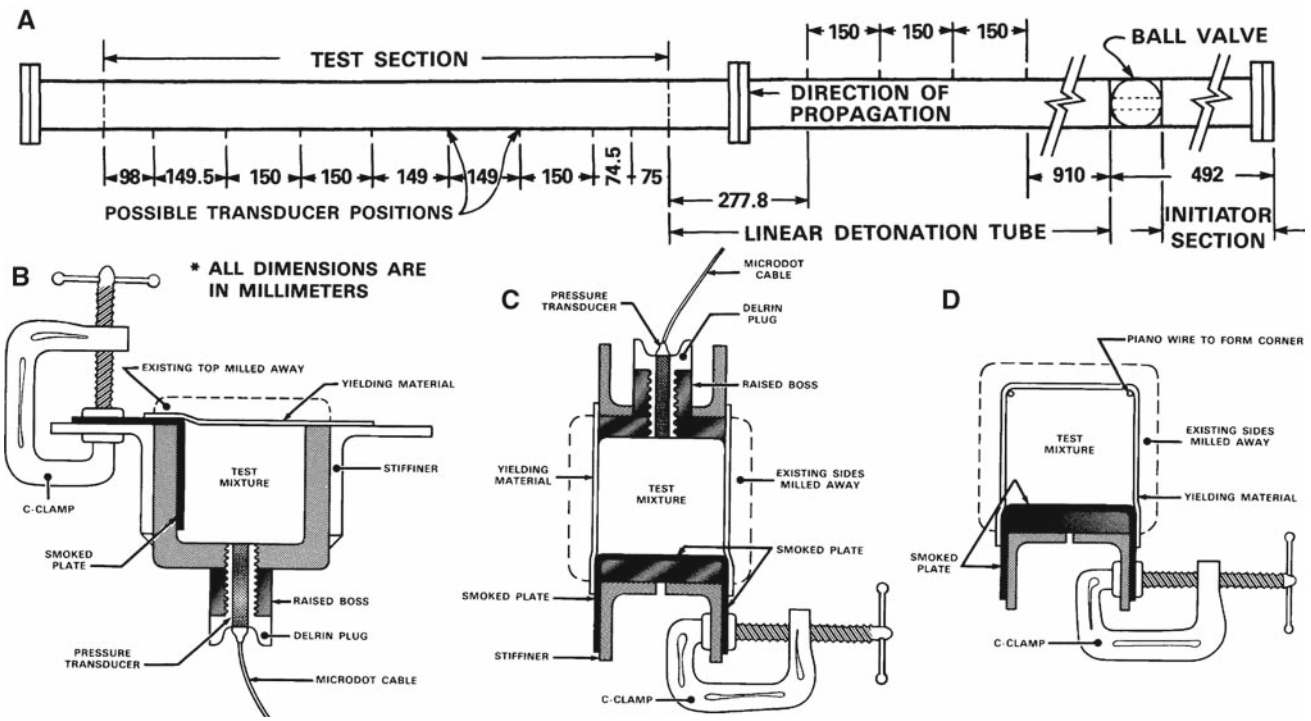

Fig. 9 Apparatus used to investigate critical conditions and velocity deficits resulting from yielding confinement. A schematic diagram of the detonation tube is shown at the *top*. Test sections with one, two, and three yielding walls are shown from *left* to *right*, respectively

Table 2 Summary of critical conditions for propagation of C_2H_2–O_2–N_2 detonations in square channels with various rigid/yielding wall configurations

Number of yielding walls	Yielding wall material	Mass of yielding wall m/A (kg/m^3)	Critical dilution ratio $\beta = [N_2]/[O_2]$	Critical cell length L_c (mm)	Critical stream tube area increase ξ (%)
1	Acetate A	0.0381	6.25	53.1	16.6
1	Acetate B	0.0351	6.25	53.1	17.3
1	Paper A	0.0372	6.13	50.0	15.4
1	Paper B	0.0616	–	–	–
1	Polyethylene	0.0831	–	–	–
2	Acetate A	0.0381	5.75	41.3	21.8
2	Paper A	0.0372	∼4.90	∼26.0	∼10.0
			(5.80)	(42.9)	(22.8)
3	Paper A	0.0372	∼4.50	∼20.7	∼10.9
			(5.30)	(32.9)	(22.7)

on the detonation wave could be regulated by varying the number of yielding walls and/or the surface density of the yielding wall material. The presence of boundary layers on the rigid surfaces introduced additional expansion. The rate of chemical reaction was again controlled by the mixture composition. The test mixture was $2C_2H_2 + 5O_2 + 5\beta N_2$ for $3.5 \leq \beta \leq 6.5$.

The diagnostic methods included pressure transducers, electronic time-interval counters to measure the mean wave velocities between adjacent transducers, and smoked foils positioned in the rigid tube and on one of the non-yielding walls. The experimental procedure was to carry out 'Go'–'No-Go' tests for a given set of boundary conditions until the critical mixture composition had been identified. Tests were then conducted with more sensitive mixtures to obtain velocity deficits under supercritical conditions.

4.2.2 Experimental results

Figure 10 shows a collection of smoke records from a channel having three rigid walls and a yielding top. The records appear in order of decreasing mixture sensitivity. The first

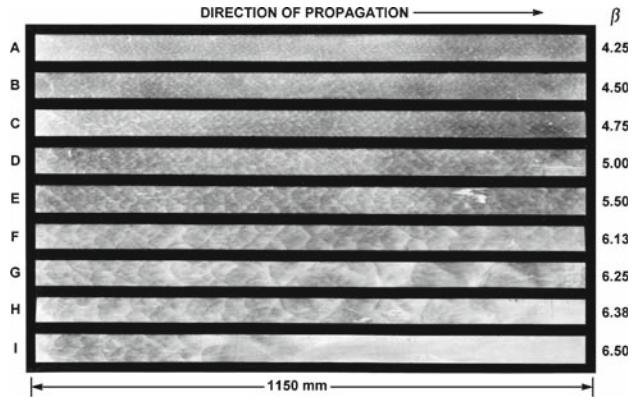

Fig. 10 Series of smoke records from a square channel having three rigid walls and one yielding acetate wall. The records appear in order of decreasing mixture sensitivity with marginal conditions apparent for $\beta = 6.25$

six records ($4.25 \leq \beta \leq 6.13$) show successful propagation from one end of the test section to the other. Absence of a cell-size gradient suggests that the wave has adjusted quickly to the new boundary conditions and has resumed steady propagation. The records labeled G through I ($6.25 \leq \beta \leq 6.50$) show that the wave is not capable of coping with the expansion once the global rate of reaction drops below some critical rate; that is, once the detonation cell exceeds some critical size. It would appear that smoke record G corresponds to critical conditions. Failure of propagation is readily apparent in smoke records H and I.

Having identified the critical compositions and corresponding cell lengths for a number of test section configurations, the critical stream tube area increases were evaluated in a manner similar to that for the large-scale tests. These are summarized in Table 2. The only difference is that the geometry is not axisymmetric, so in the calculation of ξ, each yielding wall is assumed to accelerate laterally outward and corner effects are ignored. For a single yielding wall, the results for the paraffin coated paper (Paper A) and both acetates reveal critical area increases slightly below the value of about 20% observed in the large-scale experiments. An insufficient number of tests was carried out to determine the critical conditions for a single yielding wall of either polyethylene or Paper B. For two yielding walls of Acetate A, the critical ξ is again close to 20%. However, for experiments involving two or three yielding walls of Paper A, the critical values of ξ are well below 20%. This result is consistent with the lower critical ξ determined for a single yielding wall of the same material. With this wall material, it was noted that critical conditions were not repeatable from one test to the next. The outcome was also seen to depend on the elapsed time between the termination of flowing gas and initiation, suggesting that diffusion through the wall was likely the problem. This suspicion was confirmed by the smoke records, which showed that the actual cell size was considerably larger than the anticipated one based on the known gas flow rates. Using the actual cell sizes, the calculations for these cases have been repeated. The results (bracketed quantities in the table) are in better agreement with those from the other experiments.

Under supercritical conditions, the wave propagates at a velocity, V, lower than the theoretical velocity, V_{C-J}. Figure 11 shows the experimentally measured velocity deficits, $\Delta V / V_{C-J}$, plotted against the calculated values of ξ. The scatter in the data is due partly to errors in the measurement of the wave times of arrival, particularly for cases involving oscilloscope traces. It may also be due to the three-dimensional pulsating nature of the front as critical conditions are approached. The curve through the data is again based on Dabora's rendition [6] of Fay's "nozzle" analysis [13] given by Eq. (3). The curve, plotted for $\gamma_2 = 1.2$, describes the trend of the data quite well. If we had chosen a smaller characteristic chemical kinetic length (e.g., the induction-zone length) over which to calculate ξ, the data would have fallen well below the model prediction. In contrast, had we selected the hydrodynamic thickness of the wave (i.e., ~2–4 cell lengths according to Edwards et al. [11]), the data would have resided well above the predicted results. The reasonably good correlation is a posteriori evidence that the selection of L_c as the controlling chemical kinetic length is appropriate. The maximum velocity deficit of about 10–12% apparent in Fig. 11 is in agreement with that observed in the large-scale experiments and that proposed by Edwards et al. [10] based on the Shchelkin instability criterion [36].

5 Reinterpreting the velocity deficits from Manson's students and others

If the critical ξ of 20% and the variation of $\Delta V / V_{C-J}$ with ξ are of a universal nature, they must hold true for different boundary conditions. Figure 12 shows a plot, similar to the one in Fig. 11, for the data reported by Manson's students for boundary layers in tubes, as well as the data from other authors. These data cover a wide range of mixture composition, initial pressure, geometry and mechanism responsible for the expansion. Included are the Poitiers data from Brochet [2], Boislève [1], and Renault [34], as well as the data from Edwards et al. [9] for deficits resulting from viscous boundary layers in rigid circular and rectangular tubes. To calculate ξ, the boundary layer displacement thickness, δ^*, estimated by Fay [13] using Gooderum's [14] correlation has been used: $\delta^* = 0.22\eta^{0.8}(\mu_e/\rho_0 V_{C-J})^{0.2}$ where ρ_0 and V_{C-J} are the density and velocity of the gas entering the front, and μ_e is the dynamic viscosity at the edge of the boundary layer a distance η behind the shock. The viscosity, assumed to be that at the C–J temperature, was taken from Weast and

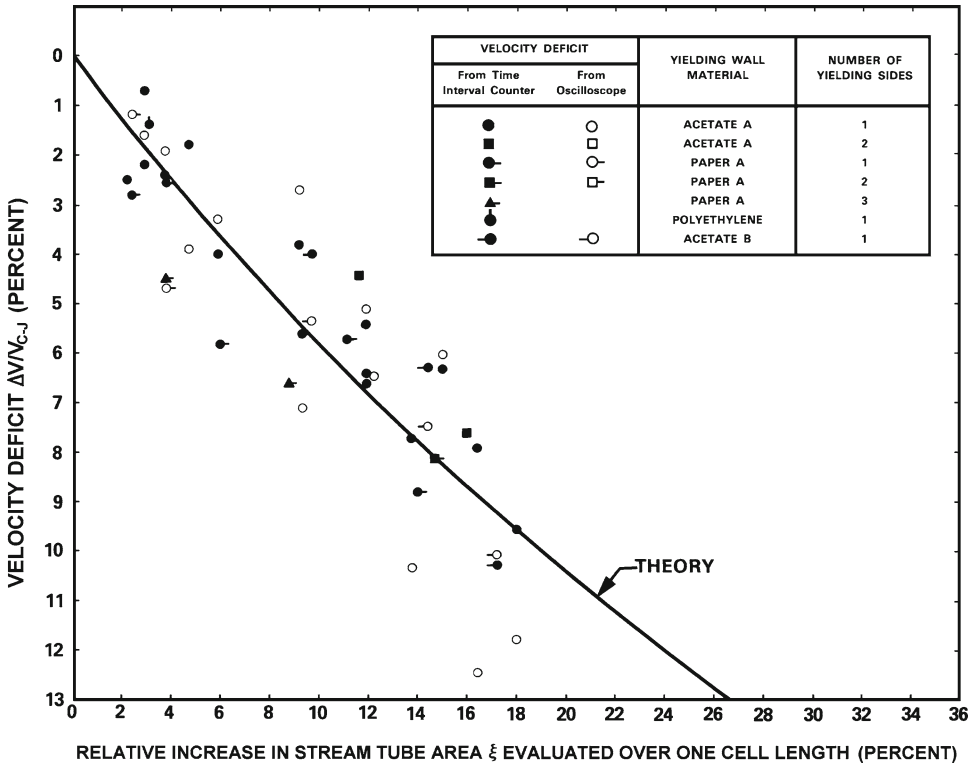

Fig. 11 Experimentally measured velocity deficits, $\Delta V / V_{C-J}$, as a function of the stream tube area increase, ξ, evaluated over one cell length, L_c, from tests in square channels with yielding walls [31,32]

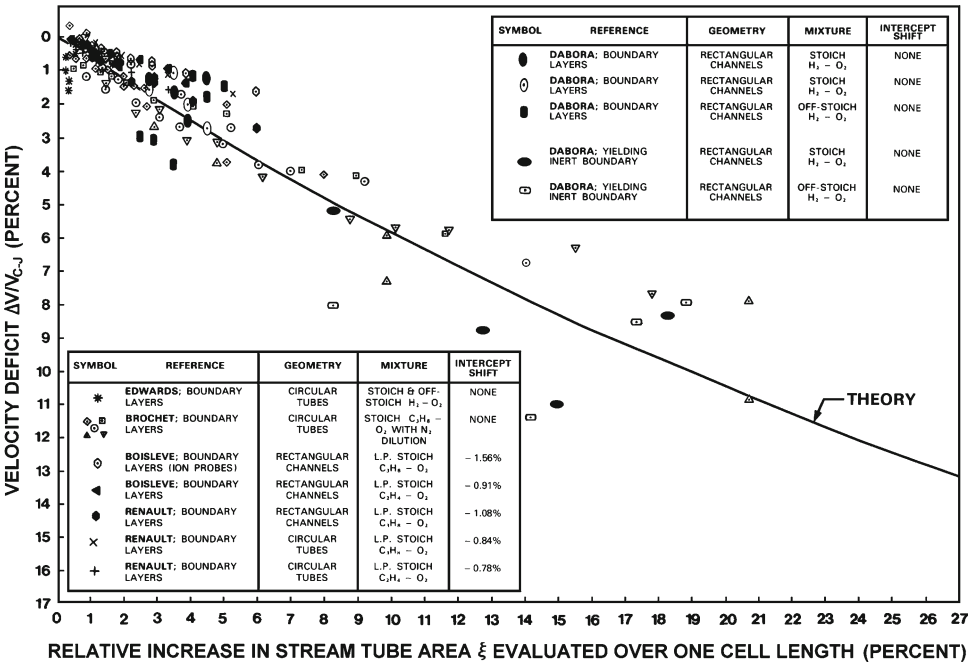

Fig. 12 Measured velocity deficits, $\Delta V / V_{C-J}$, as a function of the calculated stream tube area increase, ξ, evaluated over one cell length, L_c, based on the data for rigid tubes from Manson's students, and the data of others researchers [31,32]

Astle [39]. When data were not available for the temperature of interest, the viscosity was estimated by fitting a curve of the form suggested by Sutherland (e.g., see Chapman and Cowling [5]) to the available data and then extrapolating to the desired temperature.

When the data of Boislève [1] and Renault [34] were initially plotted, the intercept did not pass through zero as ξ tended to zero. In the plot of Fig. 12, these data have been shifted downward by a fixed amount (on the order of one percent as shown in the inset tables in the figure) deemed necessary to recover the intercept. This procedure is justified in terms of experimental error (i.e., the results of these authors for identical mixtures in identical tubes differ by about 1% due to variances in tube roughness).

The results from Dabora et al. [6] are for a rectangular column of gas bounded rigidly on three sides and by an inert compressible gas on the remaining side. For the purpose of calculating ξ, the explosive/inert interface deflection angles computed by Dabora and coworkers have been used. Boundary layer growth on the three rigid walls has also been taken into account. It should be noted that the data of Dabora et al. have been reprocessed so that the deficits are quoted with respect to V_{C-J} rather than to the measured velocity in a rigid channel of the same dimensions. In fact, two deficits have been determined from each point in the dataset of these investigators; one related to boundary layers in the rigid channel, and the other related to the compressibility of the boundary gas in conjunction with boundary layer growth on three rigid walls.

The cell sizes for low-pressure stoichiometric C_3H_8–O_2 and C_2H_4–O_2 mixtures, and for the stoichiometric H_2–O_2 mixture at atmospheric pressure, were estimated from the 13λ correlation using the critical tube diameter data of Matsui and Lee [27]. The 13λ correlation was also employed for the stoichiometric C_3H_8–O_2–N_2 system at atmospheric pressure, but using the critical tube diameter data of Knystautas et al. [18]. To the author's knowledge, no cell size data are available for off-stoichiometric H_2–O_2 mixtures at atmospheric pressure. Estimates have therefore been made based on the stoichiometric H_2–O_2 cell size and the assumption that the ratio of cell size to induction-zone length is independent of composition. The induction-time formula of Schott and Kinsey [35] has been used for this purpose.

As was the case in Fig. 11, the theory of Fay [13] describes the trend of the data in Fig. 12 quite well. The maximum $\Delta V/V_{C-J}$ and ξ of about 10 and 20%, respectively, are in agreement with those from Fig. 11, adding support to the author's proposal that the critical conditions and behavior of detonation under supercritical conditions may be of a universal nature.

6 More recent velocity deficit studies

Since the author conducted the above-described studies, there have been a number of investigations casting uncertainty on the idea of universal detonation behavior. Moen et al. [29], for example, measured velocity deficits in rigid circular tubes containing mixtures characterized by cellular structures having varying degrees of regularity. Results were obtained for stoichiometric C_2H_2–O_2 mixtures highly diluted with argon (high regularity), for stoichiometric C_2H_6–O_2 mixtures (poor regularity), and for C_2H_2–air and C_2H_4–air mixtures (irregular). The tests with fuel–air mixtures were performed at atmospheric pressure, while those involving fuel–oxygen mixtures were done at sub-atmospheric pressure. The stainless steel tubes were relatively small in these experiments, ranging in diameter from 4.7–12.7 mm. As shown in Fig. 13, the velocity deficit data were found to be in good agreement with the predictions based on Fay's model for the argon-diluted mixtures with highly regular cellular structures. However, there was a discrepancy between the experimental results and the model predictions that increased as the cellular structure became more irregular. The mixture sensitivity in this study was expressed by the ratio of the mixture's critical tube diameter to the tube diameter used in the actual tests. Very small velocity deficits, in the 1–3% range, were reported for fuel–air mixtures with irregular structures. These authors proposed that irregular cellular structures are associated with detonations having a wider spectrum of combustion instabilities that allow the wave to adjust more easily to the gasdynamic modes imposed by the boundary conditions.

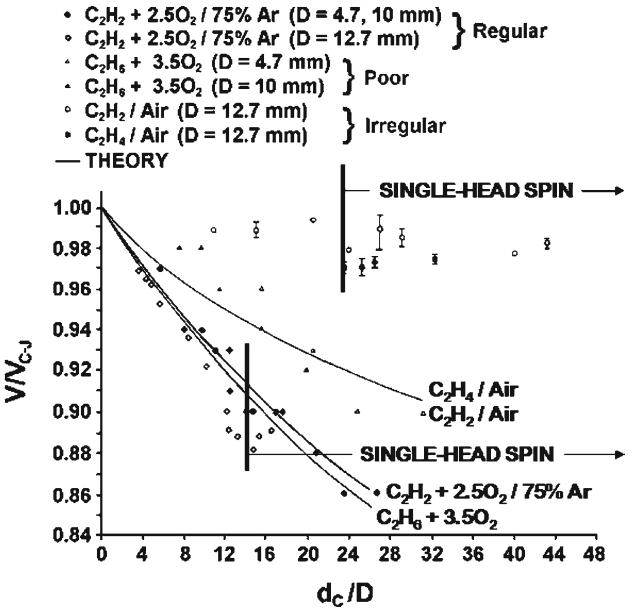

Fig. 13 Detonation velocity, V/V_{C-J}, versus mixture sensitivity, d_c/D, for mixtures having different levels of cellular regularity as reported by Moen et al. [29]. The solid curves are calculations based on the Fay-Dabora model [6,13]; reproduced with permission of DRDC Suffield

Laberge et al. [19] later studied propagation of detonation at sub-atmospheric pressures in tube bundles consisting of glass tubes 1.69, 5.46, and 11.55 mm in diameter. Figure 14, taken from Laberge [19], shows the data of Moen et al. [29] for circular tubes and those of Vandermeiren and Van Tiggelen [38] for rectangular tubes (32 mm x 92 mm). In both cases, the mixtures were stoichiometric acetylene–oxygen having a high degree of argon dilution (~70–80%). For the purposes of this comparison, an equivalent hydraulic diameter was calculated for the rectangular tubes. The data from both investigations are in good agreement, and Fay's model is seen to describe the trend of the data quite well for these mixtures exhibiting highly regular cellular structures.

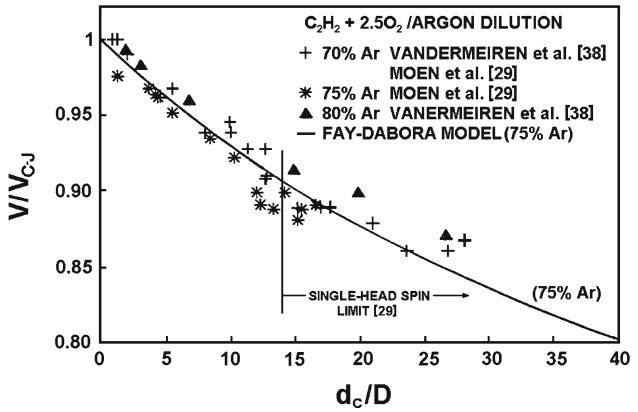

Fig. 14 Measured detonation velocity, V/V_{C-J}, versus mixture sensitivity, d_c/D, in single smooth-walled tubes and channels for stoichiometric acetylene–oxygen mixtures highly diluted with argon [19]; reproduced with permission of the American Institute of Astronautics and Aeronautics

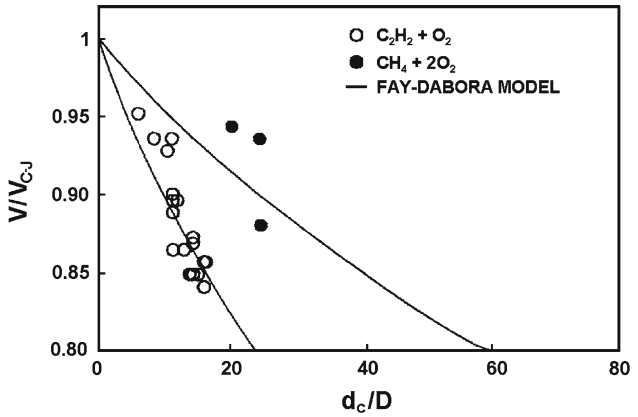

Fig. 15 Measured detonation velocity, V/V_{C-J}, versus mixture sensitivity, d_c/D, in smooth-walled glass tube bundles for equimolar acetylene–oxygen and stoichiometric methane-oxygen [19]; reproduced with permission of the American Institute of Astronautics and Aeronautics

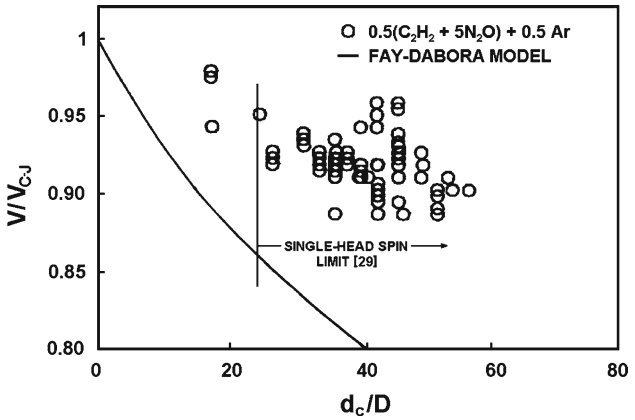

Fig. 16 Measured detonation velocity, V/V_{C-J}, versus mixture sensitivity, d_c/D, in smooth-walled glass tubes for a detonable mixture characterized by a highly irregular cellular structure [19]; reproduced with permission of the American Institute of Astronautics and Aeronautics

The maximum velocity deficit of 15% is only slightly larger than that apparent in Figs. 11 and 12.

Figure 15 shows a similar plot for undiluted equimolar C_2H_2–O_2 and stoichiometric CH_4–O_2 mixtures from the tube-bundle tests of Laberge et al. [19]. Laberge described these mixtures as having "fairly regular" structures. Fay's model once again describes the data trends quite well. The maximum velocity deficit is approximately 15% for the acetylene–oxygen system, but is somewhat smaller (∼12%) for the methane–oxygen system. The situation is quite different for a mixture of $0.5(C_2H_2 + 5N_2O) + 0.5Ar$, as shown in Fig. 16. This mixture is characterized by highly irregular cellular structures. As can be seen in the figure, there is no correlation between the experimental data and Fay's model. This finding is consistent with that of Moen et al. [29]. However, unlike Moen's results, there is significant scatter in the data, with the deficits reaching values as high as 13% in some cases.

On the surface, the above conclusions appear to contradict the results of the yielding wall experiments conducted by the author. All of his experiments involved C_2H_4–air mixtures or C_2H_2–O_2 mixtures with high N_2 dilution (i.e., irregular structures), yet Fay's model appeared to be quite applicable. However, there are a number of factors, apart from cellular regularity, that might explain the differences. In the case of the field experiments with yielding polyethylene tubes, the critical conditions for the 1, 5 and 10 mil thick walls corresponded to D/λ values of 9.9, 5.4 and 4.1, respectively. For the square channels, the critical conditions corresponded to $W/\lambda \cong 2$ for the channel with only one yielding wall. More cells were present under critical conditions for two and three yielding walls. Therefore, the velocity deficits under supercritical conditions obtained in both sets of experiments were for situations in which multiple cells were present across the tube or channel. One might expect Fay's model to be valid under these circumstances. This was not the case for Moen's experiments employing fuel–air mixtures in tubes. In those tests, most of the data are for mixtures corresponding to single-head spin or mixtures less sensitive.

Moen et al. [29] reported that the onset of single-head spin in 12.7-mm tubes occurred for $d_c/D \cong 14$ for C_2H_2–O_2–Ar mixtures and for d_c/D in the 24–27 range for C_2H_2–air mixtures. These spin limits have been added to Figs. 13 and 14 for clarity. It is apparent that most of the data for the argon-diluted mixtures is for multi-headed detonations, while most of the data for the fuel–air mixtures is for single-head spin conditions. So, although the mixtures do have very different degrees of cellular regularity, the mode numbers present in the various sets of experiments are also very different. A similar conclusion can be drawn about Laberge's results. The

tubes used by Laberge cover a similar range of diameters as the tubes in Moen's study, and the mixtures are described as being "irregular" in both cases. Therefore, the onset of single-head spin likely occurs for a similar value of d_c/D in both systems. Moen's spin limit for irregular cellular structures has been added to Fig. 16. It is evident that the majority of Laberge's data are for mixtures less sensitive than that corresponding to the onset of single-head spin. Under such conditions, the shock dynamics and flow are highly three-dimensional and shock/boundary layer interactions are likely dominant.

The boundary conditions in the author's experiments are also quite different than those in the studies of Moen and Laberge. In the case of the yielding wall experiments, the expansion imposed on the reaction zone is due primarily to the wall motion. Boundary layer effects are small, particularly in the case of the field experiments. In contrast, the tubes used by Moen et al. and Laberge et al. were very small, and the expansion is a result of the displacement thickness of the boundary layer. However, in addition to imposing a flow divergence, the boundary layer likely interacts with the transverse wave system in a complex fashion. The fact that the velocity deficits for the fuel–air detonations in Moen's experiments are virtually independent of mixture composition (even for conditions above the spin limit) also suggests that the effective reaction-zone length of the detonation is being governed by some other phenomenon. Perhaps, turbulence has dominated the combustion processes in these small tubes. The small magnitude of the velocity deficits might be explained by either a shortening of the reaction zone, or maybe a decreased flow divergence because the laminar-to-turbulent transition distance becomes significant for these small smooth tubes. It would be worth reworking Fay's theory, but taking into account the transition distance, to see if this could explain the small deficits reported by Moen et al.

A final difference between the author's yielding wall experiments and the rigid tube experiments is the nature of the wall itself. Lee [21] has suggested that the polyethylene material used in the yielding wall experiments may have the effect of dampening the transverse waves. The observation that the plastic tube breaks up into long strips corresponding approximately to the cell width [31] suggests that transverse wave mechanical energy is indeed being imparted to the walls. Weaker transverse waves are a characteristic of the regular cellular structures for which Moen et al. found Fay's model to be applicable.

There is no question that cellular regularity affects the dynamic behaviour of detonation waves. Moen et al. have found that transmission of detonation through an annular orifice is significantly enhanced for irregular cellular structures [29]. They have also shown that the 13λ correlation breaks down for low-pressure acetylene–oxygen mixtures with high argon dilution. The latter has been confirmed by Lee [20]. Desbordes [8] has reported a similar result for oxyacetylene mixtures highly diluted with monatomic inert gases. Given these observations, it is likely that the cellular regularity will also have an influence on the velocity deficits. However, more work is needed to clarify this influence. On the one hand, the author's results for multi-headed detonations in yielding tubes are in general agreement with predictions from Fay's model. On the other hand, the data of Moen et al. and Laberge et al. for single-head spin in small tubes are inconsistent with Fay's model. The mixtures used in all of these studies were characterized by irregular cellular structures. The apparent discrepancies in the results could be clarified by repeating Moen's or Laberge's experiments with larger rigid tubes (i.e., for reduced viscous effects) and/or by repeating the author's yielding tube experiments with heavier walls (i.e., for lower mode numbers).

7 Concluding remarks

Professor Manson made significant contributions to the understanding of detonation stability and velocity deficits in rigid tubes. He and his students measured the velocities in various sizes of circular and rectangular tubes and used these data to estimate the detonation velocity for an infinite tube by plotting the detonation velocity against the reciprocal of the tube diameter and extrapolating the straight line through the data points to $\phi^{-1} = 0$ (infinite tube diameter). Manson was also one of the early investigators to shed light on the cellular structure of detonation by recording and trying to interpret the origins of the striations seen in streak schlieren photographs.

The author has extended Manson's work by investigating propagation of detonation in tubes and channels having yielding walls. Whereas boundary layers were responsible for the gasdynamic expansion and related velocity deficits in Manson's rigid tubes, it was the moving boundaries that caused similar effects in the author's investigations. With the benefit of a more detailed understanding of the cellular structure of detonation waves, the author has repeated the "nozzle" analysis of Fay and Dabora using the cell length as the relevant chemical kinetic length scale to estimate the velocity deficits resulting from moving boundaries. This approach gave reasonably good agreement between the experimental results and the model. When the modified model was applied to the data obtained by Manson's students and other investigators, it was seen to describe the trends quite well.

There is experimental evidence that the model is not applicable to detonations with highly irregular cellular structures. However, much of the dissenting data were obtained for low mode numbers in small tubes. Further work is required to more fully assess the role of cellular regularity on the critical conditions and velocity deficits for gaseous detonations.

References

1. Boislève, J.N.: Propagation des détonations dans des mélanges gazeux contenus dans des tubes de section rectangulaire. Ph.D. thesis, University of Poitiers, Poitiers, France (1970)
2. Brochet, C.: Contribution a l'étude des détonations instables dans les mélanges gazeux. Ph.D. thesis, University of Poitiers, Poitiers, France (1966)
3. Brossard, J., de Coysevox, N.C.: Effets d'un confinement souple sur la détonation des mélanges gazeux. Acta Astronaut **3**, 971–981 (1976)
4. Campbell, C., Woodhead, D.: The ignition of gases by an explosion wave. Part I. Carbon monoxide and hydrogen mixtures. J. Chem. Soc. p. 1572 (1927)
5. Chapman, S., Cowling, T.: The mathematical theory of non-uniform gases 3rd edn. Cambridge University Press, London (1970)
6. Dabora, E., Nicholls, J., Morrison, R.: The influence of a compressible boundary on the propagation of gaseous detonations. In: Proceedings of the 10th Symposium (International) on Combustion, pp. 817–830. Combustion Institute, Pittsburgh (1965)
7. Denisov, Y., Troshin, Y.: Pulsating and spinning detonation of gaseous mixtures in tubes. Dokl. Akad. Nauk SSSR (Phys.-Chem. Sec) **125**, 110 (1959)
8. Desbordes, D.: Failure of the classical dynamic parameters relationships in highly regular cellular detonation systems. Prog. Astronaut. Aero. **153**, 347–359 (1993)
9. Edwards, D., Jones, T., Price, B.: Observations on oblique shock waves in gaseous detonations. J. Fluid Mech. **17**, 21–32 (1963)
10. Edwards, D., Thomas, G., Nettleton, M.: The diffraction of a planar detonation wave at an abrupt area change. J. Fluid Mech. **95**, 79 (1976)
11. Edwards, D., Thomas, G., Phillips, D.: The location of the Chapman-Jouguet surface in a multiheaded detonation wave. J. Phys. D Appl. Phys **9**, 1331–1342 (1976)
12. Eyring, H., Powell, R., Duffey, G., Parlin, R.: The stability of detonation. Chem. Rev. **45**, 69 (1949)
13. Fay, J.: Two-dimensional gaseous detonations: Velocity deficit. Phys. Fluids **2**, 283 (1959)
14. Gooderum, P.: An experimental study of the turbulent boundary layer on a shock tube wall. Tech. Note 4243, NACA (1958)
15. Hidaka, Y., Kataoka, T., Suga, M.: A shock-tube investigation in ethylene-oxygen-argon mixtures. Bull. Chem. Soc. Jpn. **49**, 2166–2170 (1974)
16. Jones, H.: A theory of the dependence of the rate of detonation of solid explosives on the diameter of the charge. Proc. R. Soc. Lond. A **189**, 415 (1947)
17. Kistiakowsky, G., Knight, H., Malin, M.: Gaseous detonations. V. Nonsteady waves in CO–O_2 mixtures. J. Chem. Phys **20**, 994 (1952)
18. Knystautas, R., Lee, J., Guirao, C.: The critical tube diameter for detonation failure in hydrocarbon-air mixtures. Combust. Flame **48**, 63–83 (1982)
19. Laberge, S., Atanasov, M., Knystautas, R., Lee, J.: Propagation and extinction of detonation waves in tube bundles. Prog. Astronaut. Aero. **153**, 381–396 (1992)
20. Lee, J.: Dynamics of exothermicity. Gordon and Breach Publishers, NY (1995)
21. Lee, J.: The detonation phenomenon. Springer, Germany (2008)
22. Libouton, J.C., van Tiggelen, P.: Influence of the composition of the gaseous mixture on the structure of detonation waves. Acta Astronaut. **3**, 759 (1976)
23. Manson, N.: Sur la structure des ondes explosives dites hélicoidales dans les mélanges gazeux. Acad. des Sci. **222**, 46 (1946)
24. Manson, N., Brochet, C., Brossard, J., Pujol, Y.: Vibratory phenomena and instability of self-sustained detonations in gases. In: Proceedings of the 9th Symposium (International) on Combustion, pp. 461–469. Academic Press, New York (1963)
25. Manson, N., Guénoche, H.: Effect of charge diameter on the velocity of detonation waves in gas mixtures. In: Proceedings of the 6th Symposium (International) on Combustion, pp. 631–639. Reinhold Publishing, New York (1957)
26. Manson, N., Strehlow, R.: Discussion on detonations. In: Proceedings of the 13th Symposium (International) on Combustion, pp. 1178–1180. Combustion Institute, Pittsburgh (1970)
27. Matsui, H., Lee, J.: On the measure of the relative detonation hazards of gaseous fuel-oxygen and air mixtures. In: Proceedings of the 17th Symposium (International) on Combustion, pp. 1269–1280. The Combustion Institute, Pittsburgh (1979)
28. Mitrofanov, V., Soloukhin, R.: The diffraction of multifront detonation waves. Sov. Phys. Dokl. **9**, 1055 (1965)
29. Moen, I., Sulmistras, A., Thomas, G., Bjerketvedt, D., Thibault, P.: The influence of cellular regularity on the behaviour of gaseous detonations. Prog. Astronaut. Aero. **106**, 220–243 (1986)
30. Moen, I., Thibault, P., Funk, J., Ward, S., Rude, G.: Detonation length scales for fuel-air explosives. Prog. Astronaut. Aero. **94**, 55–79 (1984)
31. Murray, S.: The influence of initial and boundary conditions on gaseous detonation waves. Ph.D. thesis, McGill University, Montreal, Quebec (1985)
32. Murray, S., Lee, J.: The influence of physical boundaries on gaseous detonation waves. Prog. Astronaut. Aero. **106**, 329–355 (1986)
33. Pujol, Y.: Contribution a l'étude des détonations par le méthode inverse. Ph.D. thesis, University of Poitiers, Poitiers, France (1968)
34. Renault, G.: Propagation des détonations dans des mélanges gazeux contenus dans des tubes de section circulaire et de section rectangulaire: Influence de l'état de la surface interne des tubes. Ph.D. thesis, University of Poitiers, Poitiers, France (1972)
35. Schott, G., Kinsey, J.: Kinetic studies of hydroxyl radicals in shock waves. II. Induction time in the hydrogen-oxygen reaction. J. Chem. Phys. **29**, 1177–1182 (1959)
36. Shchelkin, K.: Two cases of unstable combustion. Sov. Phys. J.E.T.P. **9**, 416 (1959)
37. Strehlow, R.: The nature of transverse waves in detonations. Astronaut. Acta **14**, 539 (1969)
38. Vandermeiren, M., Van Tiggelen, P.: Cellular structure of detonation of acetylene–oxygen mixtures. Prog. Astronaut. Aero. **94**, 104–117 (1984)
39. Weast, R., Astle, M.: CRC Handbook of Chemistry and Physics. CRC Press, Boca Raton (1979)
40. White, D.: Turbulent structure of detonation. Phys. Fluids **4**, 465 (1961)
41. Zeldovich, Y.B.: On the theory of the propagation of detonation in gaseous systems. Sov. Phys. J.E.T.P. **10**, 542 (1940)